

CT
 : 5 32 20 , 5 , 4 ,
 3 . 5 , 2
 26 . 4
 16 1 19 , 8
 CT , CT
 : , 8.7 mm
 4 - 15 mm (65%) (35%) . 46%
 가 , 68%
 CT 3 12 , 6
 ,
 가 .
 :
 가 ,
 가

(parotid gland) 3%

가 CT

(1).

(2-4),

(5-7).

(fine needle aspiration biopsy)

가 (8).

5 32 .
 (nonspecified benign inflam-
 matory lymphadenopathy) 20 , 5 ,
 4 , 3 16 51
 36.8 20 , 12
 20

14 (70%) 10 , 19 , 8 CT
(50%)
12 ,
1 10 CT
, 4 5
16 (angiosarcoma), 1
2 6 1
가
Sequoia 512 (Acuson,
Mountain View, CA, U.S.A.) 15L8W

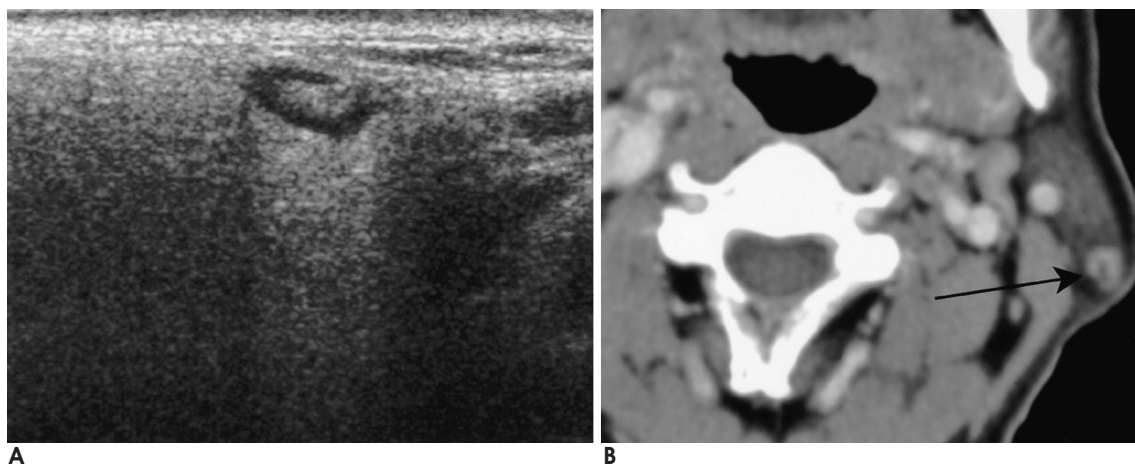


Fig. 1. Nonspecified benign inflammatory lymphadenopathy in a 26-year-old woman.

A. Longitudinal sonogram of the left parotid gland shows a well-marginated, elliptical, small hypoechoic nodule in the superficial lobe. Note the associated large area of hilar echogenicity and posterior sonic enhancement.

B. Post-contrast CT scan shows a well-defined enhancing nodule (arrow) located superficially in the left parotid gland. Note low density located somewhat eccentrically within nodule, suggesting normal fatty hilum.



Fig. 2. Cytologically proved nonspecified benign inflammatory lymphadenopathy in an 18-year-old woman.

A. Longitudinal sonogram of the right parotid gland shows a well-marginated, ovoid, small hypoechoic nodule (arrow), devoid of normal hilar echogenicity.

B. Post-contrast CT scan shows a well-defined enhancing nodule (thick arrow) in the superficial lobe of right parotid gland. Note another separate intraparotid lymph node in the retromandibular area (not proven)(thin arrow).

C. Follow-up sonogram obtained two weeks later reveals the decreased size of the node, compared with that shown in A.

1 가
 . CT Somatom Plus - S (Siemens,
 Erlangen, Germany) 100 mL
 (Omnipaque 300, Amersham Health, Cork, Ireland)
 5 mm

(posterior sonic enhancement)
 (central echogenic complex)

CT

가

Table 1. US and Color Doppler US Findings of Intraparotid Nonspecified Benign Inflammatory Lymphadenopathy

	Findings	Number of Lymph Nodes
US (n = 26)	Shape	
	rounded	9 (35%)
	oval shape	17 (65%)
	Echogenicity (in comparison with normal parenchyma)	
	hypoechoic	26 (100%)
Doppler US (n = 19)	iso or hyperechoic	0 (0%)
	Central echogenic complex	
	present	12 (46%)
	absent	14 (54%)
	Central vascularity	13 (68%)
	Peripheral vascularity	0 (0%)
	No vascularity	6 (32%)

, 5 , 2
 26
 CT
 mm 8.7 mm , (65%) 4 - 15
 가 (35%)

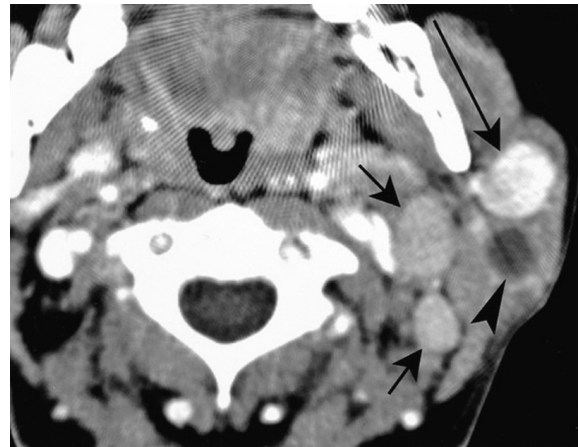


Fig. 3. Intraparotid metastases from stomach cancer in a 46-year-old woman.

Transverse CT scan obtained after injection of contrast material shows two masses in the left parotid gland. Homogeneous strong enhancement is seen in the more anteriorly located mass (long arrow) and central low attenuation with peripheral enhancement in more posteriorly located mass (arrowhead). Also noted are multiple, enhancing lymph nodes (short arrows) in the ipsilateral neck.

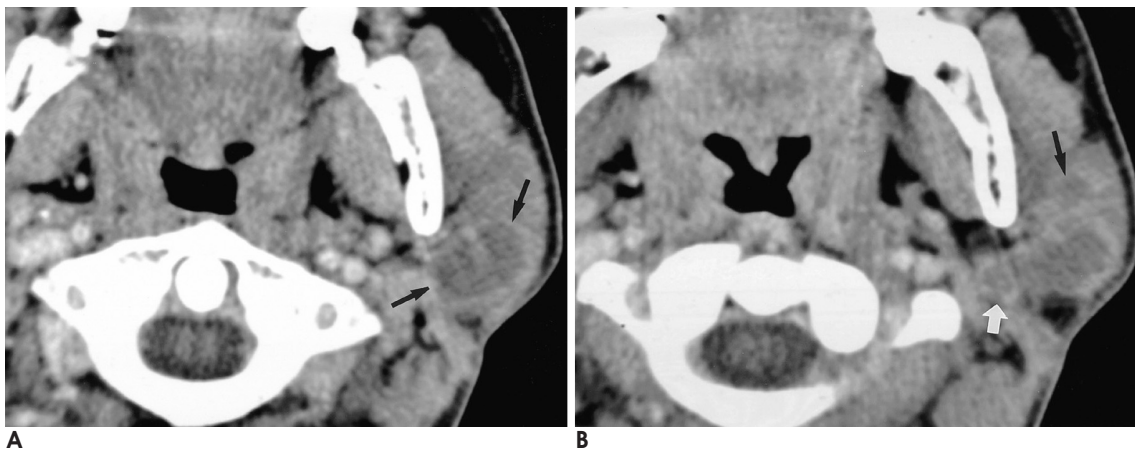


Fig. 4. Intraparotid tuberculosis in a 24-year-old woman.

A. Transverse CT scan obtained after injection of contrast material shows an ill-defined mass (arrows) with central low attenuation and faint peripheral enhancement in the left parotid gland. Note peripheral rim enhancement.

B. Transverse CT scan obtained just below A, shows another smaller necrotic lymph nodes within (black arrow) and outside (white arrow) the parotid gland.

가 12 (46%), 14 (54%)
 가 (Fig. 1, 2).
 19 13 (68%)
 , 6 (Table 1). CT mm 13 mm 4
 8 7
 , 4
 3
 (central hilum) (Fig. 1, 2).
 4 mm 1 CT
 5 3
 CT
 5 - 23 mm 13 mm 2 CT
 3
 가
 1

가 (Fig. 3).
 4 2
 10 - 21
 (Fig. 4).
 3 1
 1
 8 - 30 mm
 15 mm 3
 (Fig. 5). 3
 (Table 2).

Table 2. Enhancement Patterns of Various Intraparotid Lymphadenopathies on Contrast-Enhanced CT

	Enhancement Patterns		
	Homogeneous	Homogeneous Except Central Hilum	Peripheral
NBIL (<i>n</i> = 8*)	4	3	-
Metastasis (<i>n</i> = 5)	2	-	3
TB (<i>n</i> = 4)	-	-	4
Lymphoma (<i>n</i> = 3)	3	-	-

NBIL: Nonspecified benign inflammatory lymphadenopathy

TB: Tuberculous lymphadenitis

* Not visible on CT in 1 patient.

(parotidectomy)
 1 - 14 8
 0 - 2
 (2 - 4).
 CT

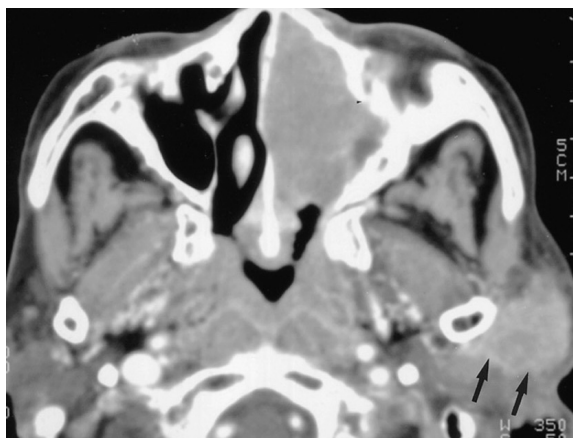


Fig. 5. Intraparotid lymphoma in a 48-year-old woman. Transverse CT scan obtained after injection of contrast material shows a large, irregular, well-enhancing soft tissue mass (arrows) in the left parotid gland. A large, destructive soft tissue mass in the left maxillary sinus and soft tissue fullness in the nasopharynx are also seen.

가
 16
 가
 가
 가
 1 cm
 가
 (9, 10).

가 1 가

가 (11 - 13). CT 가 (9). (encapsulation)

60% (19).

CT MR

(pleomorphic adenoma),

가 ,

가

(14).

100 가 (6),

가

35%가

가 48% (gray scale)

(20).

가

가

5%

(7).

CT 8 7

가

4 mm 1 CT 가 (21).

가

가

가

CT가

가 1 - 2%

(15, 16).

가

(17). Seifert

(5) 108 (submandibular gland)

60%

가

(melanoma),

5 4

1

5 MR

가

(18).

5 2 CT , 2

1. Som PM, Biller HF. High-grade malignancies of the parotid gland: identification with MR imaging. *Radiology* 1989;173:823-826
2. McKean ME, Lee K, McGregor IA. The distribution of lymph nodes in and around the parotid gland: an anatomical study. *Br J Plast Surg* 1985;38:1-5
3. Marks NJ. The anatomy of the lymph nodes of the parotid gland. *Clin Otolaryngol* 1984;9:271-275
4. Pisani P, Ramponi A, Pia F.J. The deep parotid lymph nodes: an anatomical and oncological study. *Laryngol Otol* 1996;110:148-150
5. Seifert G, Hennings K, Caselitz J. Metastatic tumors to the parotid and submandibular glands-analysis and differential diagnosis of 108 cases. *Pathol Res Pract* 1986;181:684-692
6. Janmeja AK, Das SK, Kochhar S, Handa U. Tuberculosis of the parotid gland. *Indian J Chest Dis Allied Sci* 2003;45:67-69
7. Balm AJ, Delaere P, Hilgers FJ, Somers R, Van Heerde P. Primary lymphoma of mucosa-associated lymphoid tissue (MALT) in the parotid gland. *Clin Otolaryngol* 1993;18:528-532
8. Layfield LJ, Tan P, Glasgow BJ. Fine-needle aspiration of salivary gland lesions: comparison with frozen sections and histologic findings. *Arch Pathol Lab Med* 1987;111:346-353
9. van den Brekel MW, Stel HV, Castelijns JA, Nauta JJ, van der Waal I, Valk J, et al. Cervical lymph node metastasis: assessment of radiologic criteria. *Radiology* 1990;177:379-384

10. Vassallo P, Wernecke K, Roos N, Peters PE. Differentiation of benign from malignant superficial lymphadenopathy: the role of high-resolution US. *Radiology* 1992;183:215-220
11. Chikui T, Yonetsu K, Nakamura T. Multivariate analysis of sonographic findings of metastatic cervical lymph nodes: contribution of blood flow features revealed by power Doppler sonography for predicting metastasis. *AJNR Am J Neuroradiol* 2000;21:561-567
12. Ying M, Ahuja A, Brook F. Gray scale and power Doppler sonography of normal cervical lymph nodes: comparison between Chinese and white subjects. *J Ultrasound Med* 2002;21:59-65
13. Na DG, Lim HK, Byun HS, Kim HD, Ko YH, Baek JH. Differential diagnosis of cervical lymphadenopathy: usefulness of color Doppler sonography. *AJR Am J Roentgenol* 1997;168:1311-1316
14. Bialek EJ, Jakubowski W, Karpiska G. Role of ultrasonography in diagnosis & differentiation of pleomorphic adenomas: work in progress. *Arch Otolaryngol Head Neck Surg* 2003;129:929-933
15. Chong VF, Fan YF. Parotid gland involvement in nasopharyngeal carcinoma. *J Comput Assist Tomogr* 1999;23:524-528
16. King AD, Ahuja AT, Leung SF, Lam WW, Teo P, Chan YL, et al. Neck node metastases from nasopharyngeal carcinoma: MR imaging of patterns of disease. *Head Neck* 2000;22:275-281
17. Som PM, Curtin HD. *Neck; Lymph nodes, Head and Neck Imaging* 4th ed. Missouri: Mosby, 2003:1871-1881, 2009
18. Horii A, Yoshida J, Honjo Y, Mitani K, Takashima S, Kubo T. Pre-operative assessment of metastatic parotid tumors. *Auris Nasus Larynx* 1998;25:277-283
19. Batsakis JG. Parotid gland and its lymph nodes as metastatic sites. *Ann Otol Rhinol Laryngol* 1983;92:209-210
20. Bhargava S, Watmough DJ, Chisti FA, Sathar SA. Case report: tuberculosis of the parotid gland-diagnosis by CT. *Br J Radiol* 1996;69:1181-1183
21. Hirokawa N, Hareyama M, Akiba H, Satoh M, Oouchi A, Tamakawa M, et al. Diagnosis and treatment of malignant lymphoma of the parotid gland. *Jpn J Clin Oncol* 1998;28:245-249

Intraparotid Lymphadenopathy: Ultrasonographic and CT Findings¹

Dae Young Yoon, M.D., Chul Soon Choi, M.D., Eun Joo Yoon, M.D., Young Lan Seo, M.D.,
Sang Joon Park, M.D., Soo-Hyun Lee, M.D., Jeung Hee Moon, M.D.

¹Department of Diagnostic Radiology, Hallym University College of Medicine, Kangdong Seong-Sim Hospital

Purpose: The purpose of this study was to evaluate the ultrasonographic and CT findings of various diseases that affect the intraparotid lymph node.

Materials and Methods: The subjects were 32 patients having various diseases involving the intraparotid lymph node. The final confirmed diagnoses were nonspecified benign inflammatory lymphadenopathy ($n=20$), metastasis ($n=5$), tuberculous lymphadenitis ($n=4$), and lymphoma ($n=3$). For the nonspecified benign inflammatory lymphadenopathy, there were multiple lesions in five patients and bilateral lesions in two patients, and a total of 26 lesions were included in this study. The pathologic proof of the diagnosis was made for 4 of 26 lesions, and by ultrasound follow-up on 22 of 26 lesions. All the patients underwent ultrasound. Color Doppler imaging was also performed in 19 patients and contrast-enhanced CT was also performed in 8 patients. All cases with metastasis, tuberculous lymphadenitis and lymphoma were pathologically confirmed and these patients were all examined with contrast-enhanced CT.

Results: For the nonspecified benign inflammatory lymphadenopathy, all the lesions were seen at the superficial lobe. All twenty six lesions were observed as well-defined ovoid or round hypoechoic nodules with posterior sonic enhancement on ultrasonography. A central echogenic hilum was seen in 12 of 26 inflammatory lymphadenopathies (46%), and a central hilar vascularity was noted in 13 of 19 inflammatory lymphadenopathies (68%) on color Doppler imaging. Contrast-enhanced CT showed well-defined nodules with homogeneous enhancement in most lesions. In 3 lesions, a central low density hilum was seen within a lymph node. In 12 cases with metastasis, tuberculous lymphadenitis and lymphoma, there were multiple lesions in 6 cases. CT revealed intraparotid masses with or without central necrosis and the associated multiple lymph node enlargements in the ipsilateral neck region, and their appearances were similar to that of parotid mass.

Conclusion: Nonspecified benign inflammatory lymphadenopathy involving intraparotid lymph nodes often demonstrated characteristic ultrasonographic findings, including a central echogenic hilum on gray scale US and central hypervascularity on color Doppler ultrasonography. In the metastatic lesions, the tuberculous lymphadenitis and the lymphomas, the multiplicity of lesions and the associated enlarged lymph nodes in the ipsilateral neck region could be helpful in the differential diagnosis.

Index words : Lymphatic system, hyperplasia
Lymphatic system, neoplasms
Parotid gland, neoplasms
Parotid gland, US

Address reprint requests to : Dae Young Yoon, M.D., Department of Radiology, Kangdong Seong-Sim Hospital,
Hallym University College of Medicine, 445 Gil-dong Kangdong-gu, Seoul 134-010, Korea.
Tel. 82-2-2224-2312 Fax. 82-2-488-7370 E-mail: evec0914@chollian.net